Large-scale Analysis of Trajectory Interaction Networks in Europe

Raúl López-Martín and Massimiliano Zanin
Instituto de Física Interdisciplinar y Sistemas Complejos CSIC-UIB,
Campus Universitat de les Illes Balears, E-07122 Palma de Mallorca, Spain
{raullopez, mzanin}@ifisc.uib-csic.es

***Abstract*—A challenging and open topic in air traffic management is the understanding of how aircraft interact between them to avoid separation losses, consequently creating downstream effects that go well beyond single pairs. We here present a concise modelling technique of such interactions and of their propagations, based on complex network representations of the same. By relying on some basic hypotheses, we show how this method can efficiently scale and be used to represent all flights crossing the European airspace in one day. We then use this methodology to study the resulting structures in three case studies: the normal dynamics in Europe, the impact of COVID-19 on it, and an hypothetical scenario involving free flight trajectories. Among other results, we show how these structures are a function of the main traffic flows, but not of the individual flights, and are hence an emergent property of the system; how COVID-19 impacted traffic beyond what expected from a simple reduction in traffic; and how geodesic trajectories actually dampen the propagation of interactions. We further discuss open questions and possible venues for future research.**

***Keywords*—Aircraft trajectories; interactions; complex networks.**

I. Introduction

Amidst the increasing volumes of traffic that most air transport systems are experiencing in the last decades, the quest for increasing the efficiency of air navigation without impacting safety stands out as a major goal. The cornerstone of air traffic control is currently the concept of sectors, i.e. predefined regions of the airspace where a controller is in charge of directing traffic flows. While this concept has worked well for decades, it also leaves little space to improvement. Alternative solutions have been explored, including flight-centric operations [1], i.e. a decentralised approach in which each flight is controlled by the same air traffic controller throughout its entire trajectory; flow-centric operations [2], in which flight trajectories are organised in a way that reduces conflicts between them; and free flight operations [3], [4], in which aircraft have freedom of manoeuvre. In all these cases, efficiency can be increased by delegating part of the separation management, either to pilots or to automated systems; and this in turn requires identifying "easy" flights, i.e. flights that will take part in no conflicts, or in conflicts whose resolution will not cascade into additional conflicts.

Predicting such future interactions is nevertheless not easy. Conflicts can involve more than two aircraft at the same time; and the resolution of one conflict may create a new one, i.e., what is known as downstream effects [5]. Additionally, such derived conflicts may depend both on the choices made to solve the original one; and on local conditions, e.g. winds, that may affect the trajectories. Finally, as ubiquitous in air traffic, future trajectories themselves are highly uncertain.

Not surprisingly, different attempts have been made to create systems and models able to forecast such interactions and downstream consequences; some leading to crucial results, such as proving that implemented safety measures may not avoid certain collisions when downstream effects are not considered [6]. Methods have been proposed to generate optimal deconflicted trajectories, e.g. through neural networks [7], [8] or complex network metrics [9], also in the presence of unmanned autonomous vehicles [9], [10]. Interactions and downstream effects are also used to quantify the complexity of the airspace, including aspects such as the possibility of reaching deconflicted configurations [5], finding key conflicting aircraft [11], and using interaction networks to evaluate how strongly interactions propagate [12]. In spite of some interesting results, these contributions are hindered by high computational costs, limiting the scope of the analysis to small spatial and temporal scales; consequently, the global dynamics of downstream propagations has not been characterised.

In this contribution we leverage a previous work of the authors [13] to propose a large scale model of the interactions and their propagation observed in the European airspace in the last decade. The approach involves creating network representations of flights, in which each one is depicted as a node, and pairs of them are connected whenever a potential interaction is observed - i.e. whenever their distance falls below a given threshold. The resulting structures can then be analysed through the tools provided by complex networks theory [14], [15], thus providing a picture of how interactions go beyond pairs of flights. We start by introducing the methodology (Sec. II), specifically the network reconstruction process (Sec. II-A), the metrics used for the analysis of the resulting structures (Sec. II-B), and the real data required (Sec. II-D). We then propose three use cases involving the European airspace: i) the analysis of historical interactions, and of how their structure depended on the volume of traffic, from 2015 to 2019 (Sec. III); ii) the analysis of the impact of COVID-19 in 2020 and 2021, specifically focusing on how it impacted the structure of interactions (Sec. IV); and iii), the study of an hypothetical free flight scenario involving the whole European airspace (Sec. V). Results indicate that the interaction structure strongly depends

on the volume of traffic. More surprisingly, this is also strongly modulated by the day of the week; and COVID-19 impacted the observed topology beyond what expected from the traffic drop alone. We finally draw some conclusions and suggest future research topics in Sec. VI.

II. Reconstructing and analysing interaction networks

A. Reconstruction procedure

As previously introduced, the basic hypothesis of this work is that potential interactions between flights can be mapped into a complex network, which can then be analysed to describe their propagation throughout the airspace. Following this hypothesis, each flight within the studied airspace is represented by a node. Whenever the distance between two aircraft falls below a threshold, a link between the corresponding nodes is created, containing the timestamp of the event. This threshold represents the distance below which Air Traffic Control Officers (ATCOs) must pay attention to the pair of aircraft, and may intervene to change their trajectories to avoid a potential conflict. We only consider the first interaction between each pair, following the assumption that, once the ATCOs have noted and resolved any potential conflict, no further interactions among the same pair can take place; hence each pair of nodes can only be connected by one link. Additionally, no directionality is associated to the interactions; and, once a link is added, it is never removed from the network.

We illustrate this idea with a simple example - see also Fig. 1 for a graphical representation. Let us assume two aircraft flying conflicting trajectories at similar altitudes (left panel), and interacting (i.e. getting closer than a given distance threshold, see dashed circles) at time 00:30 (central panel). Due to the conflict, the trajectory of one of the aircraft is changed, and this creates a new interaction at time 00:45 (right panel). In this example, the interaction between the two initial aircraft has propagated (through its resolution) to the third vehicle.

The propagation of these potential interactions can be analysed through the paths present in the resulting network, where a path is a sequence of nodes connected by temporally-ordered links. Paths necessarily have to incorporate the temporal dimension, i.e. the timestamps of the interactions, which results in them being directed (even though links are not, as previously explained). Considering again the example of Fig. 1, there is a path, and hence a propagation, from the first to the third aircraft - the complete path will be $[1, 2, 3]$, in that order; but the path from the third to the first aircraft (i.e. $[3, 2, 1]$) cannot exist, as it would require the second aircraft to propagate the interaction backward in time.

In the present study we use a distance threshold of 10 NM, and further only accept interactions when these involve aircraft with a vertical separation of less than 2,000 ft - see Ref. [13] for an analysis of these two parameters. We have additionally imposed that each day (in UTC time) is represented by a separate network; this allows to analyse large airspaces, at the cost of losing the infrequent propagation of interactions across multiple days.

B. Analysing interaction networks

Once interaction networks have been constructed, these have been analysed through a suite of topological metrics, i.e. metrics quantifying specific aspects of the underlying structure. The considered ones are a subset of the most foundational ones available in the literature [16]; and are briefly described below for the sake of completeness.

- *Average degree*: Average number of links connecting each node, normalised by the maximum number of links connecting a single node. This is thus equivalent to the normalised average number of interactions each flight is involved in.
- *Degree entropy*: Measure proportional to the heterogeneity of the degrees of nodes [17], and calculated through the Shannon's entropy of the distribution of these. Mathematically it is defined as:

$$S = -\sum_{k=0}^{N_{max}} p(k) \ln(p(k)), \tag{1}$$

  where $p(k)$ is the proportion of flights with k interactions, and N_{max} is the maximum degree.
  Qualitatively, it states how much variety is observed in the number the interactions that each flight participates in.
- *Isolated nodes*: Number of nodes of zero degree, i.e. of flights participating in no interactions, here normalised by the total number of flights.
- *Weak giant cluster size*: Number of nodes composing the largest subset for which a path among each pair of them, in at least one direction, exists, normalised by the total number of nodes. Qualitatively this represents the largest number of flights which can pairwise (directly or indirectly) interact.
- *Efficiency*: Metric assessing how easily information can move in the network, here in terms of the propagation of interactions. It is calculated as the sum of the inverse of the distances between each pair of nodes, where the distance is the shortest path (in terms of number of links) between two nodes [18].
- *4 reachability*: Number of nodes that can be reached from a starting one through paths of length four or less. In terms of interactions, this represents the number of flights that can be affected by a source one through short propagation paths. The metric has been calculated for each node, normalised by the total number of nodes in the network, and then synthesised through the mean of the resulting distribution.
- *Reachability modularity*: The modularity of a network is a metric assessing nodes' organisation in communities [19], i.e. groups of nodes strongly connected between them and loosely connected with others. The modularity, here estimated using the Louvain algorithm [20], has

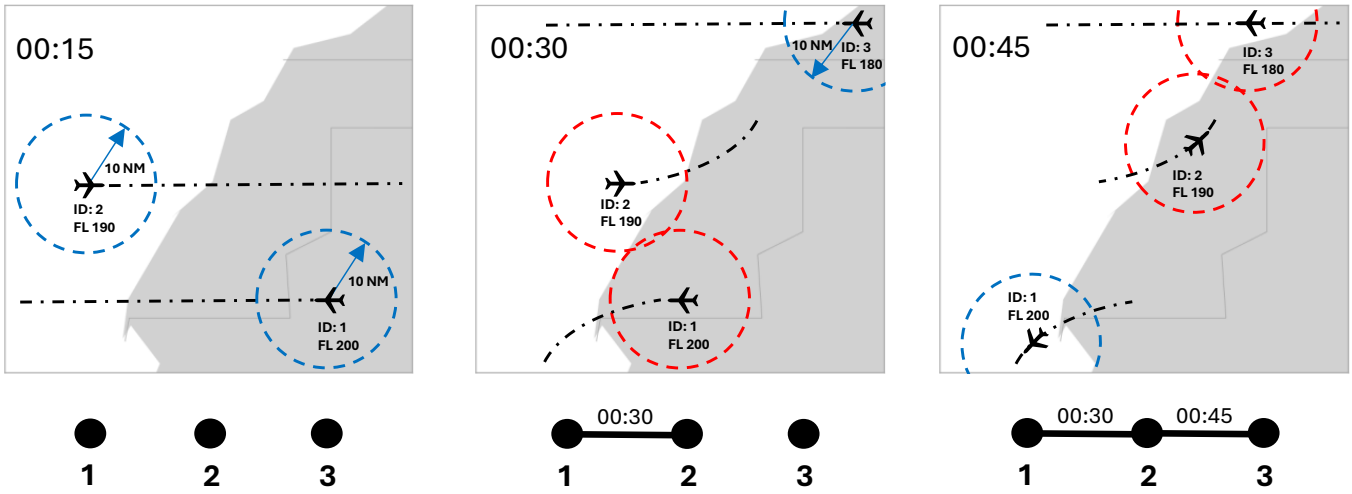

Figure 1. Graphical presentation of a simple scenario involving three aircraft, and the reconstruction of the corresponding interaction networks - see main text for details.

been calculated over a modified network representing the reachability, i.e. where pairs of nodes are directly connected whenever they are reachable through any path. This value gives an idea of how clustered, both in time and space, interactions are. The formula to calculate it is:

$$Q = \frac{1}{2m} \sum_{ij} \left(a_{ij} - \frac{k_i k_j}{2m} \right) \delta\left(c_i, c_j\right). \qquad (2)$$

a_{ij} is the ij element of the reachability matrix, and has value 1 when the ij flight pair is connected through a path in at least one direction, and 0 otherwise. Additionally, k_i is the number of other flights to which flight i is connected, and $\delta\left(c_i, c_j\right)$ takes value 1 if flights i and j belong to the same community, and 0 otherwise. m is the total number of links the network has.

Some additional topological metrics were calculated, representing variations of the aforementioned ones, but are here not reported for providing limited complementary information. These include the diameter, betweenness centrality, edge betweenness centrality [21], maximum degree, the ratio between the second and the largest degree, and the maximum 4 reachability.

C. Differences with previous work

As previously mentioned, the concept behind interaction networks is based on a previous work of the authors [13]. The reconstruction and analysis of such networks have nevertheless been overhauled focusing on the optimisation of the computations, which has resulted in a wider spectrum of analyses that can be performed.

The identification of interactions has been improved, firstly, by calculating coarse-grained versions of all trajectories, for then performing a first filter on possible interactions. This substantially reduced the number of pairs of trajectories that have to be analysed using the complete data, by excluding flights that never coincided in the same region. Secondly, the calculation of the shortest paths has been based on the algorithm proposed in Ref. [22].

This has resulted in a major reduction in the computational cost of the analyses, which in turn allowed to expand their scope. To illustrate, while the previous work was limited to the MUAC (Maastricht Upper Area Control Centre) airspace, now the full European airspace could be processed - i.e. a four-fold increase in the number of flights. Additionally, the evaluation of the obtained networks has improved, as new metrics based on shortest paths could now be computed - e.g. betweenness centrality and edge betweenness centrality. In spite of this increase in scope, the analysis of a full day of flights only takes a few hours, and could thus in principle be executed in real-time.

D. Available data

The data underpinning this work correspond to the EUROCONTROL's R&D Data Archive, a public repository of historical flights made available for research purposes and freely accessible at https://www.eurocontrol.int/dashboard/rnd-data-archive. It includes information about all commercial flights operating in and over Europe, completed with flight plans, radar data, and associated airspace structure. Data are limited at source to four months (i.e. March, June, September and December) of seven years (2015-2021). We specifically extracted the executed trajectories of each flight, and cropped them to correspond to the approximate European airspace, i.e. between $-15°$ and $30°$ in longitude, and between $35°$ and $70°$ north in latitude. We further considered the FIR and AUA versions, i.e. the trajectory points in which aircraft crossed boundaries between these air control regions, see Sec. V. Finally, the whole data set has been divided in two parts, specifically before and after March 13^{th} 2020, thus corresponding to before and after the onset of the COVID-19 pandemic.

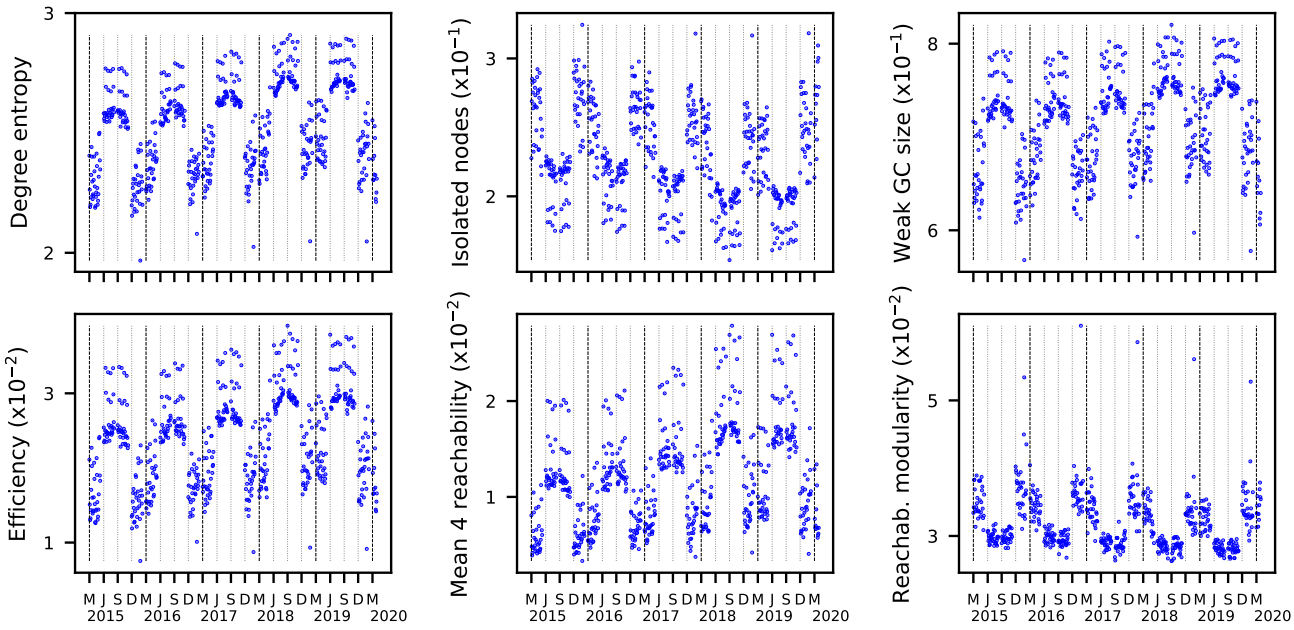

Figure 2. Evolution of the six topological metrics, across years 2015-2020, for the four months available in the data set. Each point corresponds to an individual day; thick and thin dashed vertical lines indicate respectively changes of year and month. *M*: March; *J*: June; *S*: September; *D*: December.

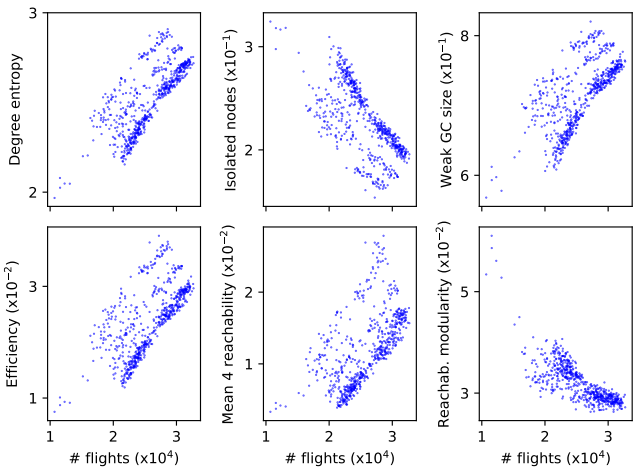

Figure 3. Scatter plots of the six topological metrics, across years 2015-2020, as a function of the daily number of flight.

III. Historical interaction structures in Europe

As a first analysis, network representations have been reconstructed for each available day prior to COVID-19, i.e. up to March 13^{th} 2020, and have further been analysed through the topological metrics described in Sec. II-B; results are depicted in Fig. 2.

A strong annual oscillation can be appreciated in all of them, with higher values during the summer season (June and September) for the degree entropy, weak GC size, efficiency, and mean 4 reachability - smaller values are in turn observed for the remainder metrics. Additionally, a similar increasing / decreasing trend is visible when considering year-to-year variations. In both cases, this suggests that the six topological metrics are highly correlated with the volume of traffic - see Fig. 3. When this hypothesis is tested using linear regression models of the individual metrics as a function of the number of daily flights, the obtained R^2 values range between 0.349 and 0.613. In other words, other variables beyond the number of flights are needed to explain the topology of the network. Other non-linear fit functions were also tested, with similar results.

A closer inspection revealed that some days of the week had a similar dynamics, irrespective of their traffic level. To illustrate, let us consider the evolution of the degree entropy (top left panel of Figs. 2 and 3): two groups of points stand out each year, especially during the summer months, corresponding to Saturdays and Sundays. When a linear fit was performed between each metric and the traffic level, but including only a specific day of the week, results substantially improved, with R^2 always above 0.8.

In order to get a more complete and quantitative picture, an analysis based on (random intercept) linear mixed models [23] has been performed. These models were fitted to reconstruct the relationship between each topological metric and the traffic level (the fixed effect), but also incorporating as random effects the day of the week, the month, and the year. In other words, they allow to express whether each one of these effects is impacting the linear model, and further provide an estimation of the statistical significance. A synthesis of these models is reported in Tab. I, specifically how the intercept is modified by each day / month / year, and the corresponding significance

TABLE I. LINEAR MIXED MODELS. ROWS REPORT THE SLOPES AND INTERCEPTS FOR THE FIXED EFFECT (TRAFFIC, OR NUMBER OF FLIGHTS); THE INTERCEPT PARAMETERS FOR THE RANDOM EFFECTS; AND THE R^2 OF THE COMPLETE MODEL. *: p-VALUE < 0.05; **: p-VALUE < 0.01.

	Degree entropy	**Isolated nodes**	**Weak giant cluster size**	**Efficiency**	**Mean 4 reachability**	**Reachability modularity**
Traffic slope (x10^{-4})	*0.208* **	*-0.038* **	*0.050* **	*0.006* **	*0.003* **	*-0.012* **
Traffic intercept	*1.805* **	*0.354* **	*0.542* **	0.002	-0.001	*0.062* **
Monday	-	-	-	-	-	-
Tuesday	-0.021	0.006	-0.010	-0.001	0.000	0.000
Wednesday	-0.023	0.007	-0.011	-0.001	0.000	0.000
Thursday	-0.017	0.004	-0.007	-0.001	0.000	0.001
Friday	-0.001	-0.001	0.001	0.000	0.000	0.001
Saturday	*0.233* **	*-0.046* **	*0.065* **	*0.009* **	*0.008* **	*-0.006* **
Sunday	*0.120* **	*-0.030* **	*0.040* **	*0.005* **	*0.003* *	-0.002
March	0.018	-0.007	0.009	0.001	0.000	-0.001
June	*0.171* **	*-0.030* **	*0.047* **	*0.006* **	*0.006* **	0.002
September	*0.168* **	*-0.029* **	*0.045* **	*0.006* **	*0.006* **	0.002
December	-	-	-	-	-	-
2015	-	-	-	-	-	-
2016	0.017	-0.001	0.003	0.001	0.001	0.001
2017	0.035	-0.003	0.006	0.001	0.002	0.001
2018	0.077	-0.012	0.017	*0.003* *	*0.004* **	0.001
2019	0.077	-0.010	0.014	*0.003* *	*0.004* **	0.002
R^2, complete model	0.955	0.938	0.930	0.944	0.905	0.800

level. To illustrate, on Saturdays the degree entropy is on average 0.233 larger than on Monday (which is taken as a reference), and this is statistically significant at 0.01 level - note how this is precisely what is intuitively described in the previous paragraph.

Tab. I indicates that the topological properties are strongly modified during Saturday and Sunday, and in June and September. This, in turn, suggests that the main drivers, beyond traffic levels, are the traffic flows in the network, i.e. which pairs of airports are connected. Note that, when all elements are included, the linear model is able to recover the metrics' values with very high precision - see the R^2 values in the last row of Tab. I. The only exception is the modularity, due to its non-linear evolution. The impact of these findings will be further discussed in Sec. VI.

IV. THE IMPACT OF COVID-19

The COVID-19 pandemic had a profound impact in our societies in general and in air transport in particular, being the restriction of movements the main tool initially used by governments to reduce the spreading of the virus. While the global impact of COVID-19 in air transport has widely been studied in the literature [24]–[27], less is known about how it affected air traffic control [28]–[30]. We are going to use the proposed methodology to ask a basic question: did COVID-19 alter flights and their interactions beyond what expected from the reduction of traffic? Or, on the other hand, was the situation comparable to days before COVID-19 with low demand?

This issue has been tackled by evaluating if and how post COVID-19 interaction networks deviated from those observed in the pre COVID-19 years. Specifically, and taking advantage of the linear tendencies found in the six metrics mentioned in Sec. III for weekday-grouped data, we compared the distribution of the residuals for pre and post COVID-19 days. In other words, we started by creating a linear fit using networks before March 13^{th} 2020, describing the evolution of each metric as a function of the number of flights; for then comparing the residuals (i.e. the errors in the fit) in the two time periods - see Fig. 4 for an example. To eliminate other confounding factors, only residuals from data that fall in a volume of traffic range present in both post and pre COVID-19 data are used - see the dashed vertical lines in Fig. 4. Additionally, Christmas days have been eliminated from the data set, as they had an anomalously low traffic throughout the data set. The distributions of the residuals of each metric, integrated across all weekdays, are depicted in Fig. 5.

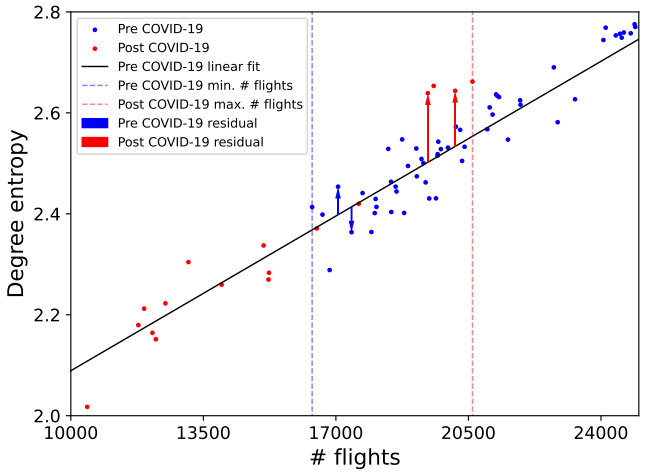

Figure 4. Scatter plot of the degree entropy as a function of the number of flights for Saturdays. Blue and red points respectively indicate pre and post COVID-19 networks, and arrows examples of the calculation of the residuals. The diagonal black line reports the best linear fit on networks before March 13^{th} 2020.

Residuals for pre COVID-19 networks are centred around zero, as is expected by construction; on the other hand, post COVID-19 ones are clearly different, as confirmed by a two-sample Kolmogorov-Smirnov test [31] - see Tab. II. In other

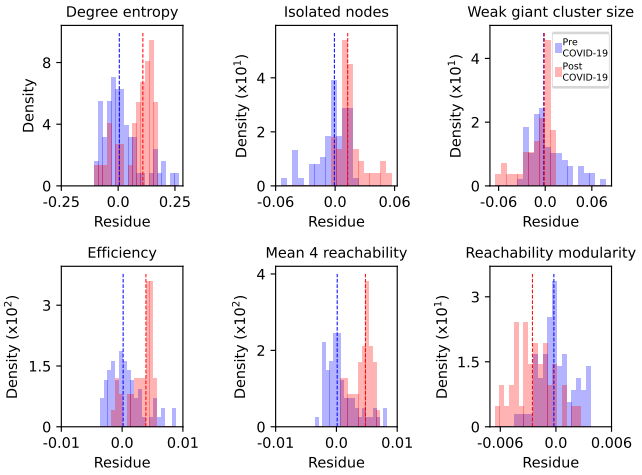

Figure 5. Histograms of the density distribution of residuals, for both the pre (blue bars) and post (red bars) COVID-19 networks, for the six considered topological metrics. Dashed vertical lines represent the median of the corresponding distribution.

words, the propagation of interactions was modified beyond what expected from a simple reduction in the number of flights, suggesting a reconfiguration of the main flows across Europe and not a simple uniform pruning [26].

The proposed analysis can also be used to explore whether a "normal dynamics" can be identified in the European air traffic; i.e. at which volume of traffic the interaction networks lose their normal structure. To this end, we calculated a linear fit for each weekday between a topological metric and the number of flights, as previously explained. Next, the residual of each day after March 13^{th} 2020 has been extracted, and normalised according to the standard deviation of the fitted values. Finally, the evolution of such residuals as a function of the ranking of the day is depicted, see Fig. 6. To illustrate, in the case of the modularity (bottom right panel), days after March 13^{th} 2020 with high volumes of traffic (thus low number in ranking, left side of the graph) have residuals close to zero, i.e. they behaved as expected in the pre COVID-19 era. A transition in most metrics can be observed around rank 130, corresponding to approx. $10,400$ flights, as indicated by the dashed vertical lines; networks with less flights (to the right of the lines) present high residuals, i.e. they deviated from the normal topology. This volume of traffic can therefore be seen as a transition point, below which the structure of the propagation network undergoes a complete breakdown.

V. Hypothetical scenario: geodesic trajectories

In order to show the usefulness of the proposed representation in the context of the evaluation of hypothetical scenarios, we here consider the case of aircraft following geodesic trajectories (direct trajectories) with different restrictions. Specifically, we compare the network representations obtained for year 2019 with those that would arise if all fights followed geodesic routes, and geodesic routes constrained by FIR and AUA (ATC Unit Airspace) structures.

TABLE II. Statistical analysis of the residuals for pre and post COVID-19 networks.

	Median pre COVID-19	**Median post COVID-19**	***p*-value**
Degree entropy	$4.49 \cdot 10^{-3}$	$1.09 \cdot 10^{-1}$	$2.38 \cdot 10^{-7}$
Isolated nodes	$-7.64 \cdot 10^{-4}$	$1.27 \cdot 10^{-2}$	$5.78 \cdot 10^{-7}$
Weak giant cluster size	$-1.85 \cdot 10^{-3}$	$-1.32 \cdot 10^{-3}$	$8.49 \cdot 10^{-3}$
Efficiency	$1.66 \cdot 10^{-4}$	$3.92 \cdot 10^{-3}$	$2.68 \cdot 10^{-7}$
Mean 4 reachability	$1.25 \cdot 10^{-4}$	$4.77 \cdot 10^{-3}$	$2.76 \cdot 10^{-11}$
Reachability modularity	$-2.20 \cdot 10^{-4}$	$-2.53 \cdot 10^{-3}$	$9.38 \cdot 10^{-7}$

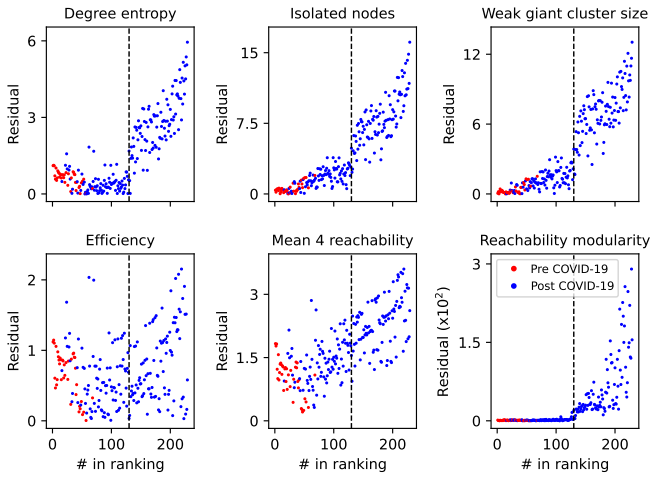

Figure 6. Scatter plots of the normalised residuals for post COVID-19 networks, as a function of their position in a ranking based on the number of flights - i.e. decreasing number of flights from left to right. Red points denote post COVID-19 days with traffic within the range of what observed before COVID-19. Vertical lines mark the 130th data point in the ranking, for visual reference.

A. Trajectories preparation

The calculation of the synthetic trajectories representing geodesic routes follows three steps.

Step 1: Horizontal trajectory: In the first step, a two-dimensional route is created, starting from the first airborne available position report and ending in the last available one. Note that these two points are not modified, to account for the initial departure and final arrival procedures, and to ensure a correct alignment with the corresponding runways. All other points are deleted, and substituted with equidistant points obtained according to the following rules:

- Full geodesic trajectory: positions are sampled across the geodesic path connecting the initial and final points.
- FIR-constrained geodesic trajectory: the position of the aircraft when crossing between two FIRs (as provided in the original data set) is preserved; the geodesic path is then calculated between these intermediate points, and new synthetic position reports are added.
- AUA-constrained geodesic trajectory: same as the previous case, but preserving the positions when crossing between two AUAs.

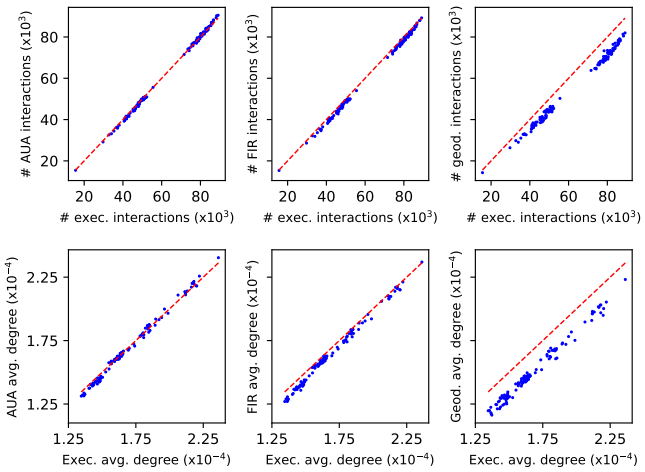

Figure 7. Scatter plots of the total daily number of interactions (top panels) and average degree (bottom panels), for the three sets of synthetic trajectories, as a function of what observed in executed ones. The red dashed lines represent the main diagonal, as a reference.

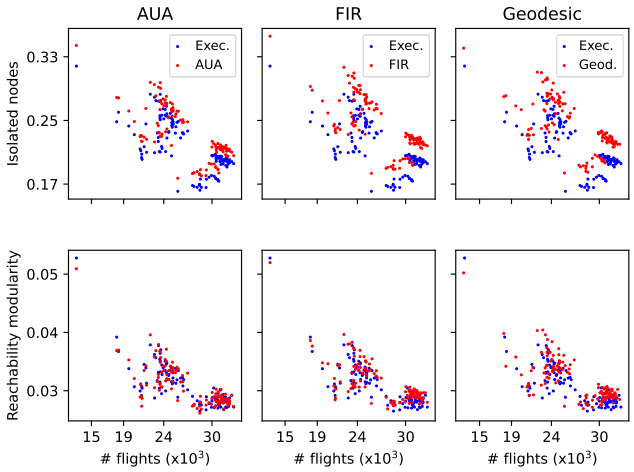

Figure 8. Scatter plots of the number of isolated nodes (top panels) and of the modularity (bottom panels), as a function of the number of flights. Blue and red points respectively correspond to executed and synthetic (see top label) trajectories.

In other words, the first version corresponds to the optimal (distance-wise) trajectory that each flight could follow; while the remainder two are restricted versions of the same, in which the hand-over points are preserved to facilitate the work of ATCOs. Consequently, being AUAs contained within FIRs, these three trajectories have increasing total distance, and decreasing difference with respect to the executed one.

Step 2: Time over: Next, a speed profile is calculated for each trajectory. For this, the original trajectory is split in two halves, and two half-profiles are calculated: the speed as a function of the time passed since crossing the initial airborne point; and the speed as a function of the time before crossing the last airborne point. In both cases, speeds correspond to ground ones, and are simply calculated as the 2D covered distance divided by the elapsed time. These speed profiles are preserved in the new trajectories, i.e. we assume that the acceleration profile does not depend on the trajectory; and they are used to calculate the time over each point.

Step 3: Vertical profiles: As a final step, the same procedure used to calculate the time over the points of the trajectory is also used to calculate the altitude. In other words, we also assume that the vertical speed of each aircraft is independent on the trajectory; and furthermore, that procedures (e.g. continuous descent) do not change.

B. Results

We start the analysis of the results by comparing the total daily number of interactions observed in each trajectory modification scenario, against what observed in real executed trajectories - see top panels of Fig. 7. Results are very similar, with a small reduction observed in the case of full geodesic trajectories (right panel); and are further confirmed when evaluating the average degree of flights (bottom panels of the same figure).

TABLE III. EXTENDED LINEAR MIXED MODELS, WITH ADDITIONAL RANDOM EFFECTS FOR AUA, FIR AND GEODESIC SYNTHETIC TRAJECTORIES. * : p-VALUE < 0.05; ** : p-VALUE < 0.01.

	AUA	**FIR**	**Geodesic**
Degree entropy	-0.010	-0.033	*-0.103* **
Isolated nodes	*0.015* *	*0.027* **	*0.025* **
Weak giant cluster size	-0.020	*-0.032* **	*-0.031* *
Efficiency	-0.001	-0.002	*-0.004* **
Mean 4 reachability	0.000	-0.001	*-0.003* **
Reachability modularity	0.000	0.001	0.001

Moving to the analysis of topological metrics, Fig. 8 reports scatter plots of the number of isolated nodes (top panels) and of the modularity (bottom panels), as a function of the number of flights; both for executed trajectories (blue points) and for synthetic ones (red points). Some important changes can be observed, especially in the case of the former and of fully geodesic trajectories. Note that this is to be expected, as the magnitude of changes in the trajectories is ordered according to AUA $<$ FIR $<$ Geodesic. We further analysed the impact on topological metrics by extending the linear mixed model of Tab. I to include the trajectory generation algorithms as random effects - see Tab. III. Note that the two metrics included in Fig. 8 corresponded to the ones yielding largest and smallest changes, respectively.

The observations indicate that the use of geodesic trajectories has a positive impact in the propagation of interactions: less flights interact, as measured by the increase in the number of isolated nodes; and those that do interact, have a more homogeneous degree. This is probably due to the fact that flights can use a larger share of the airspace, hence the probability of conflicts is reduced. Thus, even if each interaction may pose a bigger challenge for ATCOs, as flows are no longer ordered, these would be more sparse and have less of a systemic nature. As a final note, it is worth highlighting that these results are qualitatively similar to what was obtained in

the synthetic model of Ref. [13] when changing the laminarity of trajectories; while beyond the scope of the present analysis, this may indicate that the spatial distribution of the system is large enough to be simulated by a random model.

VI. Discussion and conclusion

In this contribution we have proposed an analysis of the structures created by the interactions between flights, focusing on the evolution of their properties through time and in specific scenarios. We have initially focused on the topological analysis of structures observed from 2015 to 2019, and highlighted their dependence on both volumes and flows of traffic (Sec. III); we further analysed the impact that COVID-19 had thereon (Sec. IV); and finally applied the methodology to the study of hypothetical scenarios involving different variations of free flights (Sec. V). While hitherto not common in air transport, this approach of representing interactions as complex networks can effectively be used to understand their propagations, and eventually support concepts like flight- and flow-centric operations. Beyond the specific results already discussed, some additional considerations ought to be drawn.

First of all, the fact that interaction structures strongly depend on the day of the week and the month (see Tab. I) suggests that the relevant element is the traffic patterns, i.e. which pairs of airports are connected, and not the dynamics of individual flights. In other words, while individual trajectories themselves are highly uncertain and flights can be modified by many factors, the global structure of interactions is mostly stable and predictable - in statistical physics' terms, the global structure is an emergent property of the micro-scale dynamics [32], [33]. This, on the one hand, implies that it may be interesting to identify anomalous days - here not included for the sake of conciseness; but also, on the other hand, that interaction structures cannot easily be changed by small modifications of the planning of flights, thus making their manipulation a challenging problem.

Secondly, the analysis of the data corresponding to the COVID-19 pandemic deserve some discussions. What here found suggests that the structure of interactions was altered in year 2020 beyond what would have been expected if only the number of flights was changed. In other words, interactions were modified by changes in the whole dynamics of the system - as previously reported at a global and airport [29] level. An interesting question (not here tackled due to limited data availability) remains: has the system recovered its original dynamics, or did COVID-19 change it permanently?

Thirdly, we have here illustrated how the proposed methodology can be used to probe hypothetical scenarios, focusing on a simple one in which trajectories are changed to follow geodesic paths while respecting the underlying airspace structure - see Sec. V. Not all interactions are nevertheless born equal: future versions of the model will have to take into account both their complexity and the probability of their propagation, in order to yield a more realistic picture. At the same time, it is easy to envision additional scenarios of high value and timeliness, as e.g. the study of the effects of altitude capping and re-routing to reduce CO_2 emissions.

In spite of some limitations, including for instance the need for a better understanding of the operational meaning of topological metrics, the approach here presented seems to provide already some relevant results; and we strongly believe a further analysis of the results and refinements of the model can address the aforementioned limitations, leading to new meaningful outcomes.

Acknowledgment

This project has received funding from the European Research Council (ERC) under the European Union's Horizon 2020 research and innovation programme (grant agreement No 851255). This work was partially supported by the María de Maeztu project CEX2021-001164-M funded by the MICIU/AEI/10.13039/501100011033. R. L.-M. acknowledges support from the Spanish Ministry of Science, Innovation and Universities through the grant FPU22/03765.

References

[1] I. Gerdes, A. Temme, and M. Schultz, "Dynamic airspace sectorisation for flight-centric operations," *Transportation Research Part C: Emerging Technologies*, vol. 95, pp. 460–480, 2018.

[2] M. Schultz, K. Tominaga, E. Itoh, and V. N. Duong, "Introduction of moving sectors for flow-centric airspace management," in *SIDs 2023 - Proceedings of the SESAR Innovation Days*, 2023.

[3] K. D. Bilimoria, B. Sridhar, S. R. Grabbe, G. B. Chatterji, and K. S. Sheth, "Facet: Future atm concepts evaluation tool," *Air Traffic Control Quarterly*, vol. 9, no. 1, pp. 1–20, 2001.

[4] J. M. Hoekstra, R. N. van Gent, and R. C. Ruigrok, "Designing for safety: the 'free flight'air traffic management concept," *Reliability Engineering & System Safety*, vol. 75, no. 2, pp. 215–232, 2002.

[5] M. Radanovic, M. A. P. Eroles, T. Koca, and J. J. R. Gonzalez, "Surrounding traffic complexity analysis for efficient and stable conflict resolution," *Transportation Research Part C: Emerging Technologies*, vol. 95, pp. 105–124, 2018.

[6] T. Jun, M. A. Piera, and S. Ruiz, "A causal model to explore the acas induced collisions," *Proceedings of the Institution of Mechanical Engineers, Part G: Journal of Aerospace Engineering*, vol. 228, no. 10, pp. 1735–1748, 2014.

[7] D.-T. Pham, N. P. Tran, S. Alam, V. Duong, and D. Delahaye, "A machine learning approach for conflict resolution in dense traffic scenarios with uncertainties," in *Proceedings of the Thirteenth USA/Europe Air Traffic Management Research and Development Seminar*, 2019.

[8] P. N. Tran, D.-T. Pham, S. K. Goh, S. Alam, and V. Duong, "An interactive conflict solver for learning air traffic conflict resolutions," *Journal of Aerospace Information Systems*, vol. 17, no. 6, pp. 271–277, 2020.

[9] Y. Huang, J. Tang, and S. Lao, "Cooperative multi-uav collision avoidance based on a complex network," *Applied Sciences*, vol. 9, no. 19, 2019.

[10] M. Radanovic, M. Omeri, and M. A. Piera, "Test analysis of a scalable uav conflict management framework," *Proceedings of the Institution of Mechanical Engineers, Part G: Journal of Aerospace Engineering*, vol. 233, no. 16, pp. 6076–6088, 2019.

[11] T. Koca, M. A. Piera, and M. Radanovic, "A methodology to perform air traffic complexity analysis based on spatio-temporal regions constructed around aircraft conflicts," *IEEE Access*, vol. 7, pp. 104 528–104 541, 2019.

[12] H. Wang, P. Xu, and F. Zhong, "Modeling and feature analysis of air traffic complexity propagation," *Sustainability*, vol. 14, no. 18, 2022.

[13] R. López-Martín and M. Zanin, "Propagation of interactions among aircraft trajectories: A complex network approach," *Aerospace*, vol. 10, no. 3, p. 213, 2023.

[14] S. H. Strogatz, "Exploring complex networks," *Nature*, vol. 410, no. 6825, pp. 268–276, 2001.

[15] M. E. Newman, "The structure and function of complex networks," *SIAM review*, vol. 45, no. 2, pp. 167–256, 2003.

[16] L. d. F. Costa, F. A. Rodrigues, G. Travieso, and P. R. Villas Boas, "Characterization of complex networks: A survey of measurements," *Advances in Physics*, vol. 56, no. 1, pp. 167–242, 2007.

[17] B. Wang, H. Tang, C. Guo, and Z. Xiu, "Entropy optimization of scale-free networks' robustness to random failures," *Physica A: Statistical Mechanics and its Applications*, vol. 363, no. 2, pp. 591–596, 2006.

[18] V. Latora and M. Marchiori, "Efficient behavior of small-world networks," *Phys. Rev. Lett.*, vol. 87, p. 198701, 2001.

[19] S. Fortunato, "Community detection in graphs," *Physics Reports*, vol. 486, no. 3, pp. 75–174, 2010.

[20] V. D. Blondel, J.-L. Guillaume, R. Lambiotte, and E. Lefebvre, "Fast unfolding of communities in large networks," *Journal of Statistical Mechanics: Theory and Experiment*, vol. 2008, no. 10, p. P10008, 2008.

[21] M. Newman, *Networks: An Introduction*. Oxford University Press, 03 2010.

[22] H. Wu, J. Cheng, S. Huang, Y. Ke, Y. Lu, and Y. Xu, "Path problems in temporal graphs," *Proc. VLDB Endow.*, vol. 7, no. 9, p. 721–732, 2014.

[23] J. Jiang and T. Nguyen, *Linear and generalized linear mixed models and their applications*. Springer, 2007, vol. 1.

[24] P. Suau-Sanchez, A. Voltes-Dorta, and N. Cugueró-Escofet, "An early assessment of the impact of covid-19 on air transport: Just another crisis or the end of aviation as we know it?" *Journal of Transport Geography*, vol. 86, p. 102749, 2020.

[25] X. Sun, S. Wandelt, C. Zheng, and A. Zhang, "Covid-19 pandemic and air transportation: Successfully navigating the paper hurricane," *Journal of Air Transport Management*, vol. 94, p. 102062, 2021.

[26] X. Bao, P. Ji, W. Lin, M. Perc, and J. Kurths, "The impact of covid-19 on the worldwide air transportation network," *Royal Society Open Science*, vol. 8, no. 11, p. 210682, 2021.

[27] S. Li, Y. Zhou, T. Kundu, and F. Zhang, "Impact of entry restriction policies on international air transport connectivity during covid-19 pandemic," *Transportation Research Part E: Logistics and Transportation Review*, vol. 152, p. 102411, 2021.

[28] A. Lemetti, H. Hardell, and T. Polishchuk, "Arrival flight efficiency in pre-and post-covid-19 pandemics," *Journal of Air Transport Management*, vol. 107, p. 102327, 2023.

[29] F. Olivares, X. Sun, S. Wandelt, and M. Zanin, "Measuring landing independence and interactions using statistical physics," *Transportation Research Part E: Logistics and Transportation Review*, vol. 170, p. 102998, 2023.

[30] A. Kamat and M. Z. Li, "Impacts of covid-19 on air traffic control and air traffic management: A review," *Sustainability*, vol. 16, no. 15, p. 6667, 2024.

[31] J. W. Pratt and J. D. Gibbons, *Kolmogorov-Smirnov Two-Sample Tests*. New York, NY: Springer New York, 1981, pp. 318–344.

[32] P. W. Anderson, "More is different: Broken symmetry and the nature of the hierarchical structure of science." *Science*, vol. 177, no. 4047, pp. 393–396, 1972.

[33] S. Mittal, S. Diallo, and A. Tolk, *Emergent behavior in complex systems engineering: a modeling and simulation approach*. John Wiley & Sons, 2018.